

Electronic Supplementary Information

Preparation of Samples.

MTSSL was purchased from Toronto Research Chemicals and used as received. Hydroxy-DICPO and oxo-DICPO were prepared as reported in ref.¹ Samples with concentrations in the range of 0.5 mM were prepared in 1:1 water:glycerol, degassed by freeze-pump-thaw, and flame sealed.

EPR Spectroscopy.

X-band CW spectra were recorded on a Varian E9 spectrometer. DPPH ($g = 2.0036$) was used as the g value standard. Two-pulse spin echo decays were measured on a Bruker E580 using a split-ring resonator, as previously reported.² Spin-lattice relaxation rates ($1/T_1$) at X-band between 100 and 295 K were measured as reported previously for other nitroxyl radicals.^{2,3} Relaxation rates as a function of temperature were measured at the magnetic field position that corresponds to the maximum intensity in the absorption spectrum. Single exponentials gave good fits to the recovery curves in this temperature range.

Determination of tumbling correlation times.

The lineshapes of X-band CW spectra as a function of temperature were analyzed using the NLS program⁴ to determine tumbling correlation times. Parameters required for the NLS simulations were obtained by analysis of frozen solution spectra using locally-written software (Table 1).

The anisotropy of the tumbling correlation times was less than about a factor of 3, except near the glass transition temperature. As shown in Fig. 1 the temperature dependence of the tumbling correlation times, $-10 < \log \tau < -8.5$, was in good agreement with that predicted by the Stokes-

Einstein equation; $\tau = C_{\text{slip}} \frac{V\eta}{kT}$ where C_{slip} is the slip coefficient, V is the molecular volume which was estimated as the molecular weight divided by the typical density of an organic molecule (0.9 g/cm³), k is the Boltzmann constant, T is temperature in Kelvin, and η is the dynamic viscosity of a 1:1 water:glycerol mixture.⁵ Poor fitting above $\log \tau = -8.5$ may be due to anisotropic tumbling at lower temperatures. The slip coefficients were 0.25 for MTSSL, 0.39 for oxo-DICPO, and 0.68 for hydroxy-DICPO. The variations in C_{slip} are attributed to differences in solute-solvent interaction, including hydrogen bonding.

Table 1
 g and A values and rigid lattice linewidths^a

nitroxyl	g_{xx}	g_{yy}	g_{zz}	A_{xx}	A_{yy}	A_{zz}	ΔB_{xx}	ΔB_{yy}	ΔB_{zz}
MTSSL	2.0081(2)	2.0061(2)	2.0023(1)	5.8(3)	4.7(3)	36.9(1)	7.5	7.5	6.8
oxo-DICPO	2.0093(2)	2.0058(2)	2.0023(1)	5.9(3)	4.8(3)	35.9(1)	8.0	8.0	8.0
hydroxy-DICPO	2.0094(2)	2.0059(2)	2.0023(1)	6.6(3)	5.7(3)	36.6(1)	8.0	8.0	8.4

^a A values and full width at half-height linewidths (ΔB) are in gauss

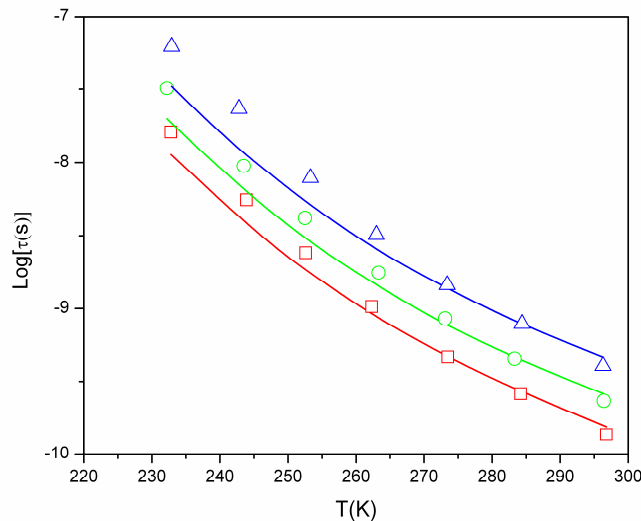


Fig. 1 Temperature dependence of tumbling correlation times, τ , for MTSSL (\square), oxo-DICPO (\circ), and hydroxy-DICPO (Δ) compared with values calculated based on the Stokes-Einstein model, including a slip coefficient (solid lines).

Modeling the temperature dependence of $1/T_1$.

The temperature dependence of $1/T_1$ was modeled by least-squares fitting with the sum of contributions from the Raman and local mode processes, spin rotation, and modulation of g and A anisotropy by tumbling,⁶ as reported previously.² The contribution from the Raman process was assumed to be in the high temperature limit and therefore proportional to T^2 . Above about 125 K the relaxation rates increase faster with increasing temperature than predicted by the Raman process, as is characteristic of a local mode. Initial data analyses gave values of the energy of the local mode between 1050 and 1130 K. The differences between these values are within the experimental uncertainties, so the average value (1090 K) was used in the final data analyses. Above the glass transition temperature (about 175 K) the relaxation rates become more strongly temperature dependent due to tumbling dependent modulation of anisotropy. The coefficients for the tumbling dependent modulation of g and A anisotropy, calculated from the g and A values shown in Table 1, are denoted as $C_{A,g}$ (theory). Since a Cole-Davidson spectral density function⁷ has been shown previously to fit well with the tumbling-dependent contribution to nitroxyl relaxation,³ it was used in this analysis. In the initial analyses values of β (the adjustable parameter in the Cole-Davidson spectral density function) were between 0.7 and 0.715 so an average value of 0.71 was used in the final parameter refinement. In the final fitting process the coefficients C_{Ram} , C_{loc} , and $C_{A,g}$ (fitting) were allowed to vary and the results are shown in Table 2. The agreement between the fit lines and the experimental data are shown in Fig. 2 and 3 for MTSSL and oxo-DICPO, respectively. The contribution from spin-rotation (which has no adjustable parameters) is negligible so it is not shown in the plots. The molar

masses of the three nitroxyl studied: MTSSL (264), oxo-DICPO (282), and hydroxy-DICPO (284) are so similar that the dependence of spin-lattice relaxation rates on effective molar volume that has been observed for nitroxyl radicals,² contributes very little to differences between these three radicals. The differences between $C_{A,g}$ (fitting) obtained from fitting the temperature dependence of $1/T_1$ and $C_{A,g}$ (theory) calculated from the known values of g , A , are within the estimated uncertainties in the input parameters. Although there was some anisotropy, geometric averages of the tumbling correlation times calculated using NLSL were used in modeling the temperature dependence of $1/T_1$. The agreement between $C_{A,g}$ (fitting) and $C_{A,g}$ (theory) indicates that the impact of anisotropy on the relaxation was not large. As was observed previously for a range of nitroxyl radicals,^{2,3} the contributions to relaxation for MTSSL, hydroxy-DICPO, and oxo-DICPO from the Raman and the local mode processes are correlated.

Table 2
 Parameters for Fitting the Temperature Dependence of $1/T_1^a$

Nitroxyl	$C_{\text{Ran}} (\text{s}^{-1})$	$C_{\text{loc}} \times 10^6 (\text{s}^{-1})$	$C_{A,g} \times 10^{16} (\text{s}^{-2})$ (theory)	$C_{A,g} \times 10^{16} (\text{s}^{-2})$ (fitting)
MTSSL	0.27	2.0	9.5	9.1
oxo-DICPO	0.24	1.6	9.0	8.5
hydroxy-DICPO	0.23	1.4	8.9	8.0

^a C_{Ran} is the coefficient of the contribution from the Raman process in the high temperature limit, C_{loc} is the coefficient of the contribution from the local mode, $C_{A,g}$ is the coefficient of the contribution from the modulation of g and A anisotropy by tumbling, where (theory) designates the value calculated from the known g and A values, and (fitting) is the value obtained by treating $C_{A,g}$ as an adjustable parameter in the least-squares fitting.

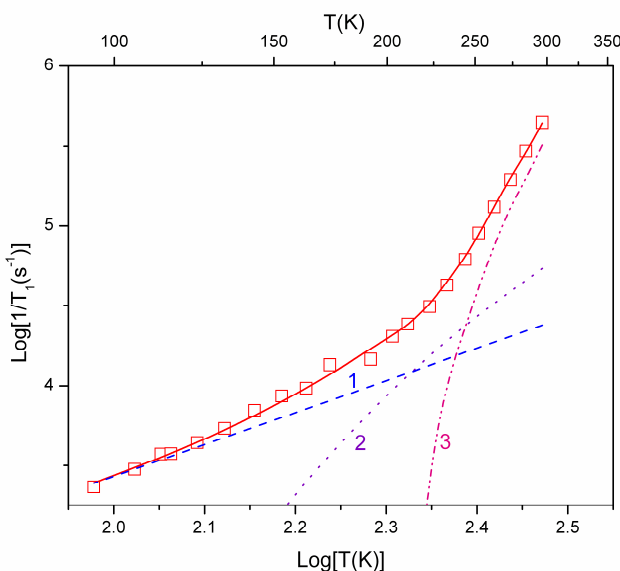


Fig. 2. Modeling of the temperature dependence of spin lattice relaxation rates for MTSSL in 1:1 water:glycerol. The solid line is the sum of contributions from the Raman process (line 1), the

local mode (line 2), and modulation of g and A anisotropy by tumbling (line 3).

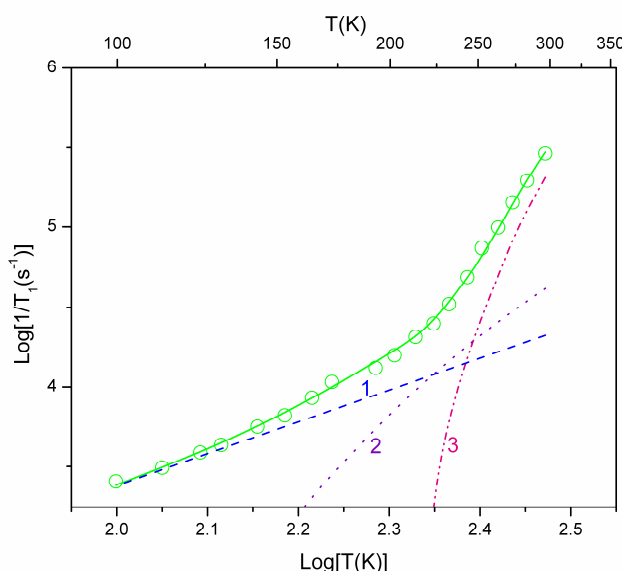


Fig. 3. Modeling of the temperature dependence of spin lattice relaxation rates for oxo-DICPO in 1:1 water:glycerol. The solid line is the sum of contributions from the Raman process (line 1), the local mode (line 2), and modulation of g and A anisotropy by tumbling (line 3).

Orientation Dependence of Relaxation Rates

The temperature dependence of spin lattice relaxation rates shown in Fig. 2 and 3 was measured in the center of the X-band spectrum and samples primarily orientations of the molecule with the magnetic field in the x,y molecular plane. Prior studies have shown that $1/T_1$ for nitroxyl radicals is dependent on the orientation of the molecule with respect to the external field.⁸ Values of $1/T_1$ at 85 K as a function of position in the spectrum are shown in Figure 4. Orientation dependence for oxo-DICPO and hydroxy-DICPO is less than for MTSSL, which is attributed to larger linewidths for the DICPO derivatives than for MTSSL which blurs out the anisotropy. The wider linewidths are attributed to unresolved proton hyperfine couplings to the spirocyclohexyl groups. For orientation dependence for $1/T_m$ at 85 K arises primarily from motion.^{6,9} The lack of orientation dependence of $1/T_m$ for oxo-DICPO and hydroxy-DICPO is consistent with expectations for negligible motion on the EPR timescale because of hydrogen bonding and rigidity of the 1:1 water:glycerol glass.

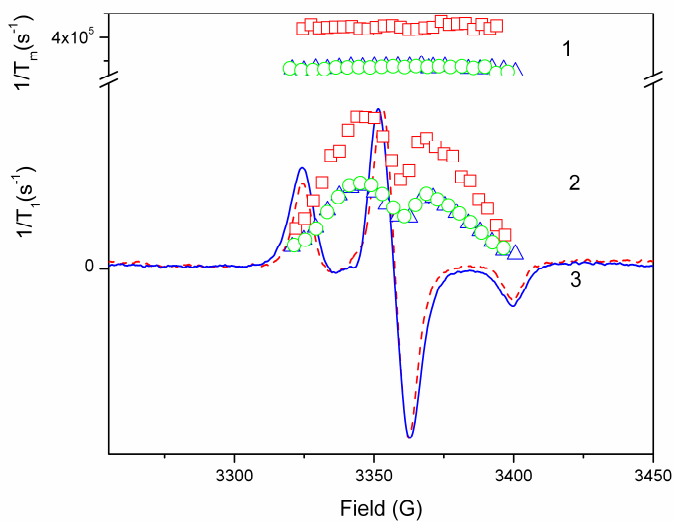


Fig. 4. Dependence of relaxation rates of nitroxyls in 1:1 water:glycerol on position in the CW spectrum at 85 K. (1) orientation dependence of spin echo dephasing rate for MTSSL (\square), oxo-DICPO (\circ), and hydroxy-DICPO (\triangle), (2) orientation dependence of electron spin lattice relaxation rate for MTSSL (\square), oxo-DICPO (\circ), and hydroxy-DICPO (\triangle), and (3) CW EPR spectrum for hydroxy-DICPO(blue solid line) and MTSSL (red broken line).

References.

1. S. Okazaki, M. A. Mannan, K. Sawai, T. Masumizu, Y. Miura and K. Takeshita, *Free Rad. Res.*, 2007, **41**, 1069-1077.
2. H. Sato, V. Kathirvelu, A. J. Fielding, S. E. Bottle, J. P. Blinco, A. S. Micallef, S. S. Eaton and G. R. Eaton, *Mol. Phys.*, 2007, **105**, 2137-2151.
3. H. Sato, S. E. Bottle, J. P. Blinco, A. S. Micallef, G. R. Eaton and S. S. Eaton, *J. Magn. Reson.*, 2008, **191**, 66-77.
4. D. E. Budil, S. Lee, S. Saxena and J. H. Freed, *J. Magn. Reson. A*, 1996, **120**, 155-189.
5. Y. M. Chen and A. J. Pearlstein, *Indust. & Engin. Chem. Res.*, 1987, **26**, 1670-1672.
6. S. S. Eaton and G. R. Eaton, *Biol. Magn. Reson.*, 2000, **19**, 29-154.
7. N. Davidson and R. H. Cole, *J. Chem. Phys.*, 1951, **19**, 1484-1490.
8. J.-L. Du, G. R. Eaton and S. S. Eaton, *J. Magn. Reson. A*, 1995, **115**, 213-221.
9. J. L. Du, G. R. Eaton and S. S. Eaton, *Appl. Magn. Reson.*, 1994, **6**, 373-378.